

# Effects of Planar Periodic Stratified Chiral Nihility Structures on Reflected and Transmitted Powers

Nayyar Abbas Shah<sup>1</sup>, Faiz Ahmad<sup>2</sup>, Aqeel A. Syed<sup>3</sup>, Qaisar A. Naqvi<sup>4</sup>

<sup>1</sup>nayyarabbas07@yahoo.com, <sup>2</sup>faizsolangi@gmail.com,

<sup>3</sup>aqeel@qau.edu.pk, <sup>4</sup>qaisar@qau.edu.pk

<sup>1,3,4</sup>Department of Electronics, Quaid-i-Azam University, Islamabad 45320, Pakistan

<sup>2</sup>Department of Physics, CIIT, Islamabad, Pakistan

## Abstract

Behavior of planar multilayer periodic structures due to plane wave excitation has been studied using the transfer matrix method. Multilayer structure is taken with periodicity two. That is, layers at even and odd locations repeat themselves. Layers at odd locations are of chiral nihility metamaterial whereas three different cases for layers at even locations are considered, i.e., dielectric, chiral and chiral nihility. Effects of polarization rotation due to the optical activity is studied with respect to the angle of incidence and frequency in terahertz domain. Chiral nihility introduces property of transparency to the structure for normal incidence while complete rejection is observed for chiral nihility-chiral nihility structure at oblique incidence .

## 0.1 Introduction

Objects in our universe can be classified in two groups: achiral and chiral. An object not superimposable to its mirror image by any translation or rotation is called chiral object. Achiral object are non-chiral and can be superposed to its mirror image [1, 2]. A metamaterial microscopically composed of chiral objects is called chiral metamaterials. The constitutive relations for isotropic, homogenous and non-diffusive chiral material are written below [3]:

$$\mathbf{D} = \epsilon \mathbf{E} + (\chi - j\kappa)\sqrt{\epsilon_0\mu_0}\mathbf{H} \quad (1)$$

$$\mathbf{B} = \mu \mathbf{H} + (\chi + j\kappa)\sqrt{\epsilon_0\mu_0}\mathbf{E} \quad (2)$$

where  $\kappa$  and  $\chi$  are chirality and non-reciprocity parameter respectively. Moreover  $\epsilon$  and  $\mu$  are permittivity and permeability representing the electric and magnetic polarizability of the material.

Lakhtakia proposed the concept of nihility metamaterial and nihility means real parts of permittivity and permeability are zero [4]. He studied the scattering of electromagnetic plane waves from a cylinder composed of nihility metamaterial [5]. Later, Tretyakov et al. extended the concept of nihility for the isotropic chiral metamaterials [6]. Chiral nihility (CN) is a special case of chiral metamaterial for which real parts of permittivity and permeability are simultaneously zero at certain frequency, i.e.,  $\epsilon \rightarrow 0$  and  $\mu \rightarrow 0$ . The constitutive relations for CN metamaterials are [6-8],

$$\mathbf{D} = -j\kappa\sqrt{\epsilon_0\mu_0}\mathbf{H} \quad (3)$$

$$\mathbf{B} = j\kappa\sqrt{\epsilon_0\mu_0}\mathbf{E}. \quad (4)$$

Several researchers have studied the behavior of metamaterial interfaces and structures when these are exposed to electromagnetic excitation. Some special arrangements using metamaterials had been proposed to fabricate absorbers, antenna radomes and cloaks [9-11]. Interaction of electromagnetic waves with chiral slabs with planar interfaces had been studied for different applications [12-14]. Rejection and tunneling of electromagnetic fields

from chiral and/or CN planar interfaces and waveguide composed of planar CN metamaterials had also been studied [15, 16]. Reflection and transmission from CN slabs embedded in other materials or backed by fractional dual interfaces are available in [17, 18]. Khalid et al. had studied scattering of electromagnetic waves from cylindrical DB boundaries in the presence of chiral and CN metamaterials [19]. Taj et al. had studied the chiral and CN metamaterials interfaces as focusing surfaces by using Maslov's method [20]. Sabah et al. had studied the behavior of multilayered structure. Sabah along with co-workers had calculated the response of the chiral mirror by using transfer matrix method (TMM) [21]. Polarization rotator by using multilayered structures had been studied by using conventional chiral and chiral metamaterial for normal incidence [22]. Planner interfaces composed of chiral metamaterials had studied for oblique incidence as filters in [23, 25].

In current paper, planar periodic multilayered structures having odd number of slabs are analyzed. Two layers form a period and it is assumed that layers at odd locations are of CN metamaterial. Three different cases are considered for layers at even locations, i.e., dielectric, chiral, and CN. Purpose of the study is to find the effects of CN metamaterial on reflected and transmitted powers.

## 0.2 Formulation

Consider planar periodic stratified structure of chiral metamaterials as shown in Figure 1. Each slab is of infinite extent in  $x$  and  $y$  directions of the Cartesian coordinate system. Slabs at odd locations have identical constitutive parameters while slabs at even locations have same values of constitutive parameters. Therefore, each slab at odd location is labeled as A whereas each slab at even location is labeled as B. It is also assumed that slab labeled A have higher value of refractive index than slab labeled B. Constitutive parameters for slab A are denoted by  $(\epsilon_H, \mu_H, \kappa_H)$  and constitutive parameters for slab B are denoted by  $(\epsilon_L, \mu_L, \kappa_L)$ . The stratified structure is placed in air medium having constitutive parameters  $(\epsilon_0, \mu_0)$ .

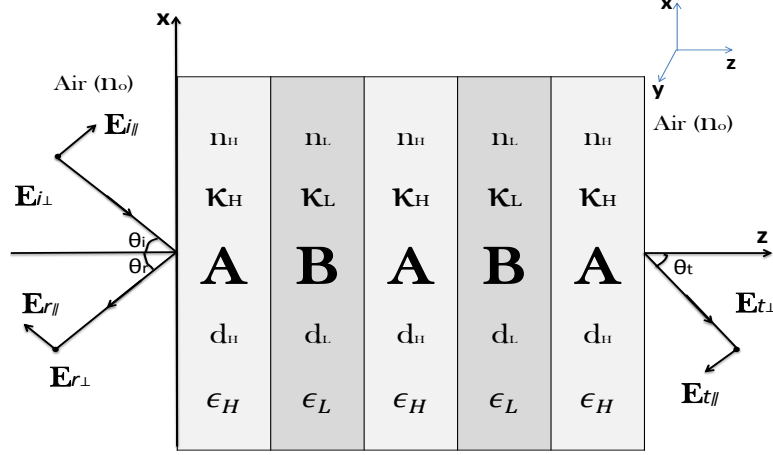


Figure 1: Stratified metamaterials at oblique incidence

The structure is excited by a parallel polarized monochromatic plane wave. The expression for incident electric field is given below:

$$\mathbf{E}_i = [E_{i||}(\hat{x} \cos \theta_i + \hat{z} \sin \theta_i)] \exp[-jk_0(z \cos \theta_i - x \sin \theta_i)] \quad (5)$$

where  $k_0 = \omega \sqrt{\epsilon_0 \mu_0}$  and  $\theta_i$  is the angle of incidence with respect to z-axis.

It is assumed that reflected and transmitted fields contain both parallel and perpendicular components. Expressions for reflected and transmitted waves, in terms of unknown coefficients, are written as

$$\mathbf{E}_r = [E_{r||}(\hat{x} \cos \theta_r - \hat{z} \sin \theta_r) + E_{r\perp} \hat{y}] \exp[-jk_0(-z \cos \theta_r - x \sin \theta_r)] \quad (6)$$

$$\mathbf{E}_t = [E_{t||}(\hat{x} \cos \theta_t - \hat{z} \sin \theta_t) + E_{t\perp} \hat{y}] \exp[-jk_0(z \cos \theta_t - x \sin \theta_t)] \quad (7)$$

$\theta_r$  and  $\theta_t$  are angles of reflection and transmission in air with respect to z-axis.

Electric and magnetic fields inside the  $m$ -th chiral slab are written as linear combination of left circularly and right circularly polarized plane waves. Both waves are propagating in forward as well as backward directions, that is, in positive and negative z-directions. Expressions for total electric field in  $m$ -th chiral slab are given below [9]:

$$\begin{aligned} \mathbf{E}_m^+ &= \mathbf{E}_{mL}^+ \exp[-jk_{mL}(z \cos \theta_{mL} - x \sin \theta_{mL})] + \mathbf{E}_{mR}^+ \exp[-jk_{mR}(z \cos \theta_{mR} - x \sin \theta_{mR})], \\ \mathbf{E}_m^- &= \mathbf{E}_{mL}^- \exp[-jk_{mL}(-z \cos \theta_{mL} - x \sin \theta_{mL})] + \mathbf{E}_{mR}^- \exp[-jk_{mR}(-z \cos \theta_{mR} - x \sin \theta_{mR})], \end{aligned}$$

with

$$\mathbf{E}_{mL}^+ = E_{mL}^+(\hat{x} \cos \theta_{mL} + \hat{z} \sin \theta_{mL} + j\hat{y}), \quad (8)$$

$$\mathbf{E}_{mR}^+ = E_{mR}^+(\hat{x} \cos \theta_{mR} + \hat{z} \sin \theta_{mR} - j\hat{y}), \quad (9)$$

$$\mathbf{E}_{mL}^- = E_{mL}^-(\hat{z} \sin \theta_{mL} - \hat{x} \cos \theta_{mL} + j\hat{y}), \quad (10)$$

$$\mathbf{E}_{mR}^- = E_{mR}^-(\hat{z} \sin \theta_{mR} - \hat{x} \cos \theta_{mR} - j\hat{y}). \quad (11)$$

Superscripts + and - are used to describe the waves propagating in forward and backward directions, respectively. Moreover  $\theta_{mL}$  and  $\theta_{mR}$  are used to describe the angles of LCP and RCP waves with respect to the z-axis. The magnetic fields outside and inside the chiral slab may be obtained from Maxwell curl equations.  $k_{mR}$  and  $k_{mL}$  are wave numbers for LCP and RCP waves, respectively and are given as,

$$k_{mL} = \omega(-\kappa_i \sqrt{\epsilon_0 \mu_0} + \sqrt{\epsilon_i \mu_i}) \quad (12)$$

$$k_{mR} = \omega(\kappa_i \sqrt{\epsilon_0 \mu_0} + \sqrt{\epsilon_i \mu_i}), \quad i = H, L. \quad (13)$$

$E_{r\parallel}$ ,  $E_{t\parallel}$ ,  $E_{r\perp}$ ,  $E_{t\perp}$ ,  $E_{mL}^\pm$  and  $E_{mR}^\pm$  are unknown coefficients to be determined using the boundary conditions. Transfer matrix method (TMM) is used to determine the reflected and transmitted fields from the planar stratified structure. First of all, matching matrices are calculated by imposing the boundary conditions at each interface. To relate fields at two consecutive interfaces, propagation matrices are also computed. Product of these matrices finally relates the reflected and transmitted fields with the incident field in form of matrix equation as given below [25],

$$\begin{pmatrix} E_{i\parallel} \\ E_{i\perp} \\ E_{r\parallel} \\ E_{r\perp} \end{pmatrix}, = T \begin{pmatrix} E_{t\parallel} \\ E_{t\perp} \end{pmatrix} \quad (14)$$

where relating transfer matrix is given below,

$$T = M_1 \cdot P_A \cdot T_1^m \cdot M_2 \quad (15)$$

$$T_1 = M_{AB} \cdot P_B \cdot M_{BA} \cdot P_A \quad (16)$$

with  $M_1$  and  $M_2$  matching matrices which relate fields across first and last interface of planar stratified structure, respectively. In general, matching matrices  $M_{ij}$  correspond to an interface with slab  $i$  on left side and slab  $j$  on right side of the interface. Propagation matrices are represented by  $P_A$  and  $P_B$  corresponding to slab A and slab B, respectively.

## 0.3 Results and Discussions

In this section, numerical results for three different structures are obtained to note the effects of CN metamaterials on transmitted and reflected powers. For all cases, parallel polarized plane wave ( $E_{i\perp} = 0$ ) is considered for incidence and structure have odd numbers of slabs. In all cases, each slab have optical width  $\lambda_0/4$  except for CN case when slabs have physical width equal to  $\lambda_0/4$ , where  $\lambda_0$  corresponds to the first harmonic frequency of  $f_0 = 1\text{THz}$ .

### 0.3.1 CN-dielectric Structure

In the first case, slabs labeled as A are of CN metamaterial whereas slabs labeled as B are of dielectric medium. It is assumed that structure is composed of five slabs. Each CN slab has physical width of  $\lambda_0/4$  and each dielectric slab have thickness  $\lambda_0/4n_d$ , where  $n_d$  is refractive index of the dielectric slab. Figure 2 describes behavior of reflected power versus frequency for normal incidence. It has sinusoidal behavior with maximum amplitude equal to 40 percent of the incident power. Reflected power approaches to zero at 1.0, 2.0, 3.0 and 4.0THz frequencies. Figure 3 shows the behavior of transmitted power versus frequency. Transmitted power has both cross and co-polarized components and these are shown by dotted and solid lines, respectively. It is also observed that rotation is  $45^\circ$  at 1.0 and 3.0THz, and complete rotation is noted at 2THz for normal incidence.

In Figure 4 and Figure 5, reflected and transmitted powers versus frequency for oblique

incidence are plotted. It is noted that total reflection is observed at higher frequencies but some ripples are also noted in the reflected and transmitted powers at lower values of frequencies.

Figure 6 shows reflected power versus angle of incidence. Total reflection is noted for  $\theta_i > 22^\circ$  for fixed frequency of 1THz. The increasing trend for co-polarized component is also observed and it takes value unity from  $\theta_i = 60^\circ$  to  $\theta_i = 90^\circ$ . Corresponding transmitted power, shown in Figure 7, has both cross and co-polarized components up to  $\theta_i = 22^\circ$  having maximum rotation at  $15^\circ$  and becomes zero for next values.

### 0.3.2 CN-CN structure

For second case, it is assumed that both slabs A and B are of CN metamaterials with same value of chirality but having different limiting values of permittivity and permeability. Physical width of each slab is equal to  $\lambda_0/4$ . In Figure 8 and Figure 9, it is observed that total power is transmitted through the structure but due to optical activity of the chiral material, the plane of polarization gets rotated. Rotation is  $90^\circ$  at 2THz frequency for the chirality parameter  $\kappa_H = \kappa_L = 0.1$ .

In Figure 10 and Figure 11, behavior of CN-CN structure is studied versus frequency for oblique incidence. For these figures,  $\theta_i = 45^\circ$  is considered and total reflection is noted after fraction of 1THz and total transmission is noted for 0.2THz.

Next two figures describe behavior of reflected and transmitted power versus angle of incidence. In Figure 12, complete reflected power is noted from  $\theta_i = 15^\circ$  to  $\theta_i = 90^\circ$  having maximum contribution of co-polarized component and cross component has largest contribution at  $\theta_i = 10^\circ$ . In Figure 13, transmitted power is observed only at lower values of angle of incidence with major contribution from co-polarized component.

### 0.3.3 CN-chiral structure

In third case, we consider that the slab at odd positions are of chiral metamaterial. Chiral slabs have optical width equal to quarter wavelength and lower chirality value than CN slabs. In Figure 14 and Figure 15, it is noted that reflected power has small percentage of incident power and transmitted power has major contribution of the cross polarized component for small values of angle of incidence. Whereas at higher degrees of incidence angle reflected power starts increasing and transmitted power shows decaying trend.

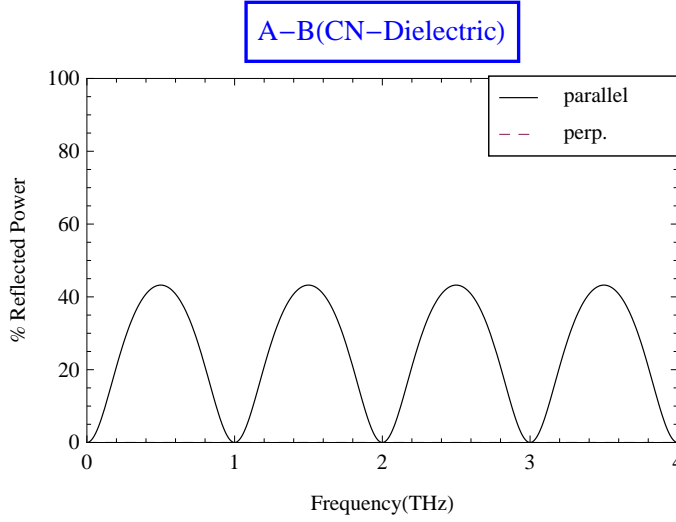


Figure 2:  $\epsilon_H = 1.6 * 10^{-4}$ ,  $\mu_H = 1 * 10^{-5}$ ,  $n_L = 2.2$ ,  $d_H = |n_L|d_L = \lambda_0/4$ ,  $\kappa_H = 0.167$



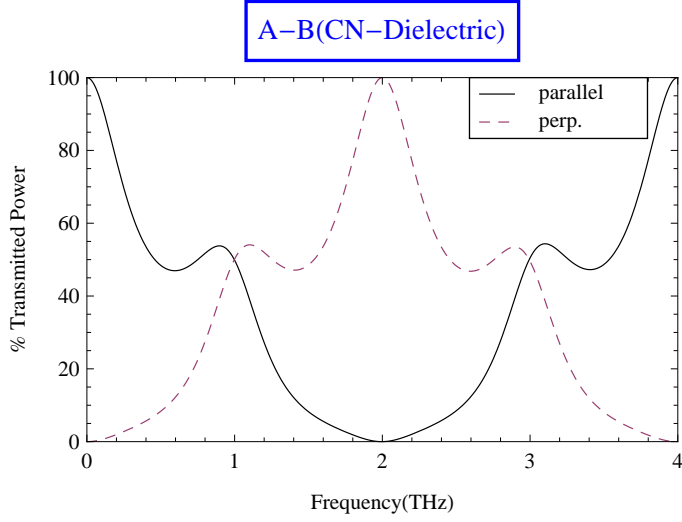


Figure 3:  $\epsilon_H = 1.6 * 10^{-4}$ ,  $\mu_H = 1 * 10^{-5}$ ,  $n_L = 2.2$ ,  $d_H = |n_L|d_L = \lambda_0/4$ ,  $\kappa_H = 0.167$

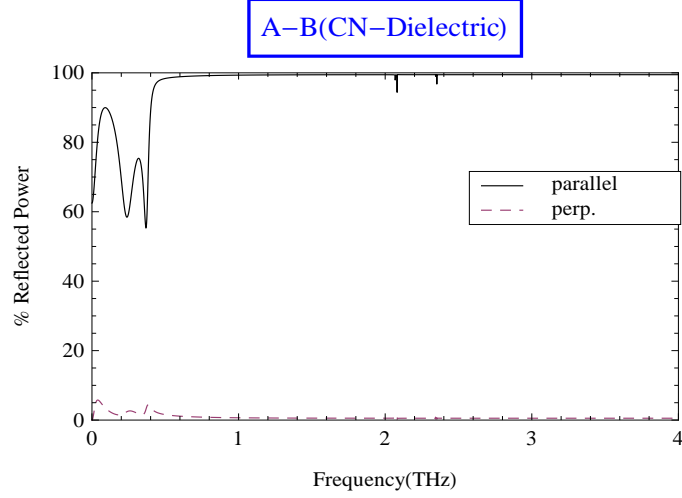


Figure 4:  $\epsilon_H = 1.6 \times 10^{-4}$ ,  $\mu_H = 1 \times 10^{-5}$ ,  $n_L = 2.2$ ,  $d_H = |n_L|d_L = \lambda_0/4$ ,  $\kappa_H = \kappa_L = \kappa = 0.1$ ,  $\theta_i = 70^\circ$

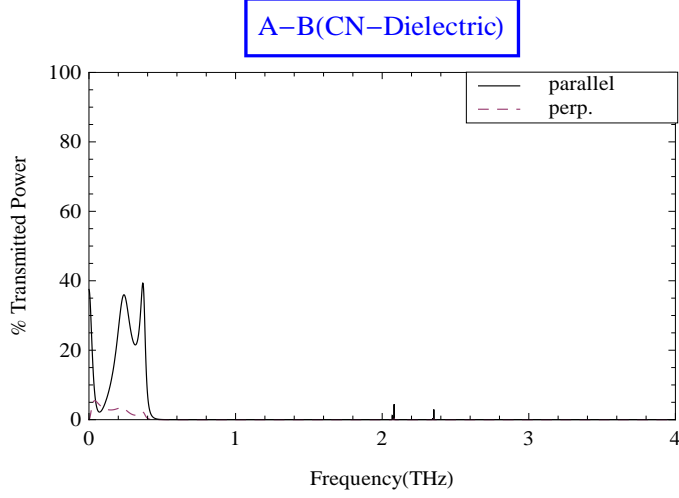


Figure 5:  $\epsilon_H = 1.6 \times 10^{-4}$ ,  $\mu_H = 1 \times 10^{-5}$ ,  $n_L = 2.2$ ,  $d_H = |n_L|d_L = \lambda_0/4$ ,  $\kappa_H = \kappa_L = \kappa = 0.1$ ,  $\theta_i = 70^\circ$

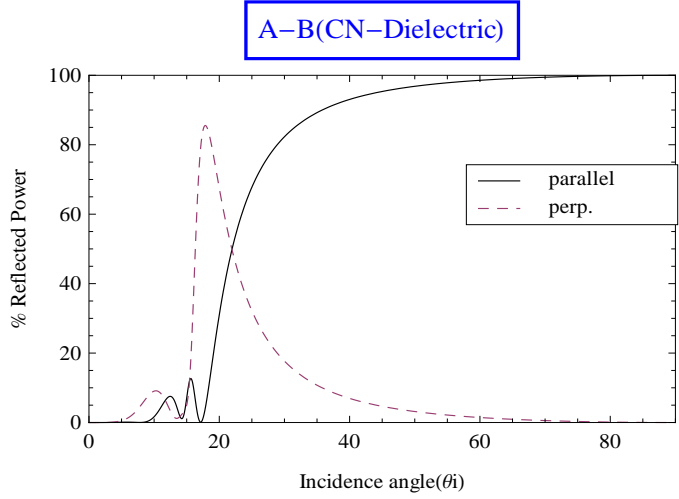


Figure 6:  $\epsilon_H = 1.6 \times 10^{-4}$ ,  $\mu_H = 1 \times 10^{-5}$ ,  $n_L = 2.2$ ,  $d_H = |n_L|d_L = \lambda_0/4$ ,  $\kappa_H = 0.1$ ,  $f/f_0 = 1$

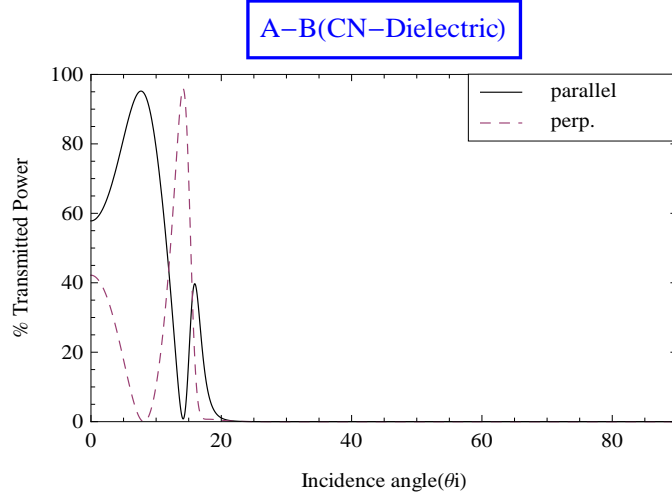


Figure 7:  $\epsilon_H = 1.6 \times 10^{-4}$ ,  $\mu_H = 1 \times 10^{-5}$ ,  $n_L = 2.2$ ,  $d_H = |n_L|d_L = \lambda_0/4$ ,  $\kappa_H = 0.1$ ,  $f/f_0 = 1$

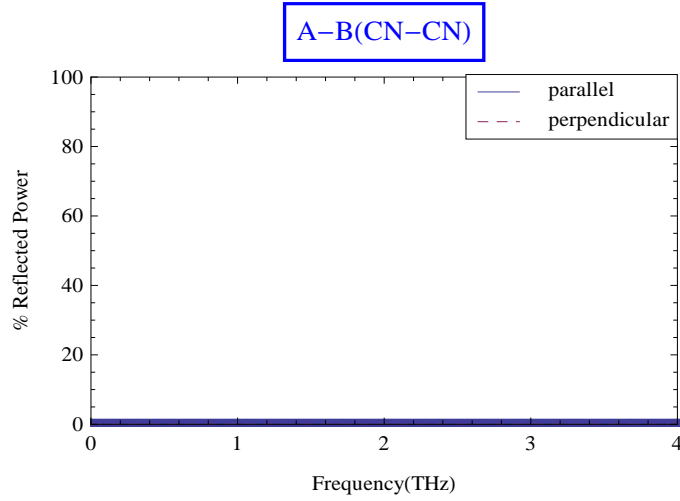


Figure 8:  $\epsilon_H = 1.6 \times 10^{-4}$ ,  $\epsilon_L = 2.5 \times 10^{-5}$ ,  $d_H = d_L = \lambda_0/4$ ,  $\kappa_H = \kappa_L = 0.1$

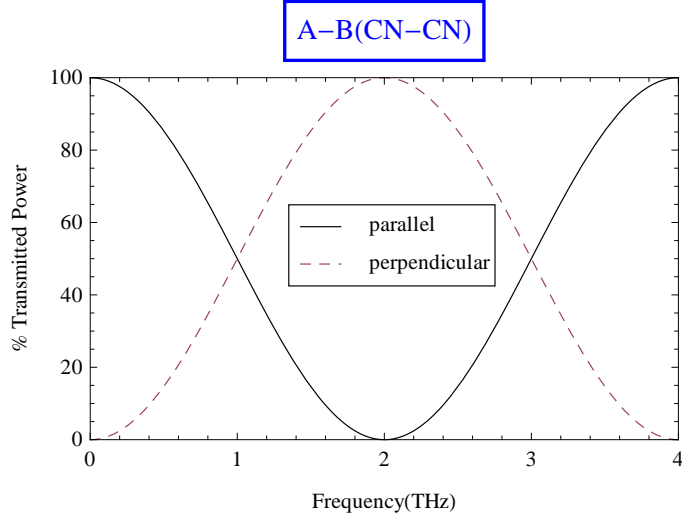


Figure 9:  $\epsilon_H = 1.6 \times 10^{-4}$ ,  $\epsilon_L = 2.5 \times 10^{-5}$ ,  $d_H = d_L = \lambda_0/4$ ,  $\kappa_H = \kappa_L = 0.1$

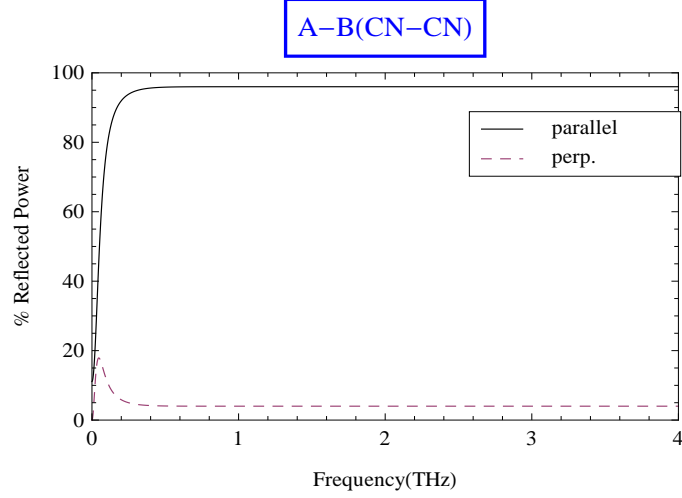


Figure 10:  $\epsilon_H = 1.6 \times 10^{-4}$ ,  $\epsilon_L = 2.5 \times 10^{-5}$ ,  $\mu_H = \mu_L = 10^{-5}$ ,  $d_H = d_L = \lambda_0/4$ ,  $\kappa_H = \kappa_L = 0.1$ ,  $\theta_i = 45$

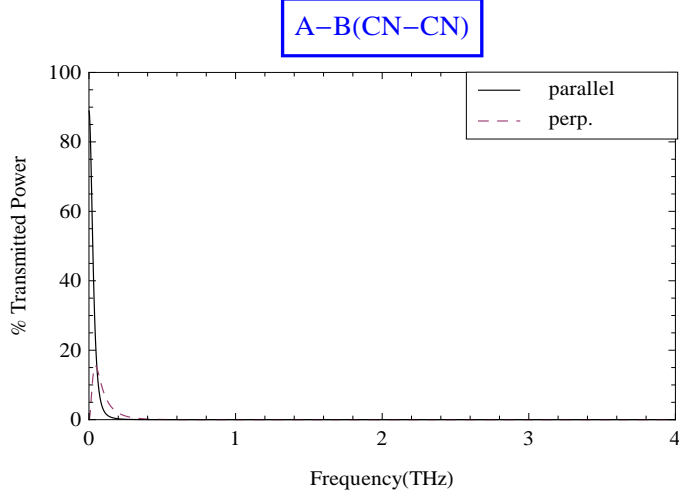


Figure 11:  $\epsilon_H = 1.6 \times 10^{-4}$ ,  $\epsilon_L = 2.5 \times 10^{-5}$ ,  $\mu_H = \mu_L = 10^{-5}$ ,  $d_H = d_L = \lambda_0/4$ ,  $\kappa_H = \kappa_L = 0.1$ ,  $\theta_i = 15$

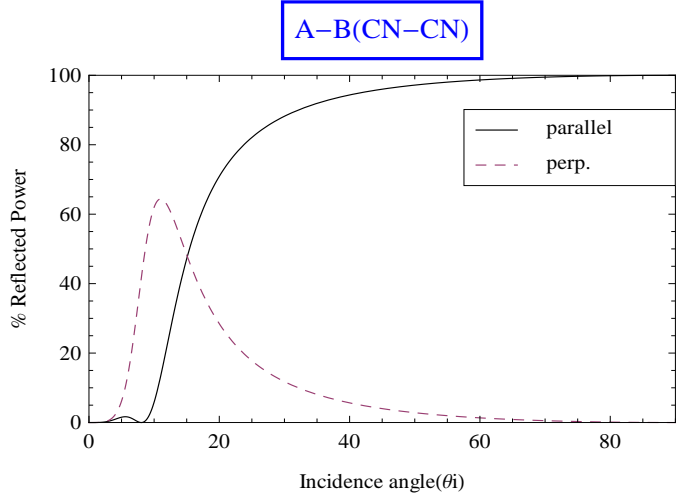


Figure 12:  $\epsilon_H = 1.6 \times 10^{-4}$ ,  $\epsilon_L = 2.5 \times 10^{-5}$ ,  $\mu_H = \mu_L = 10^{-5}$ ,  $d_H = d_L = \lambda_0/4$ ,  $\kappa_H = \kappa_L = 0.1$ ,  $f/f_0 = 1$

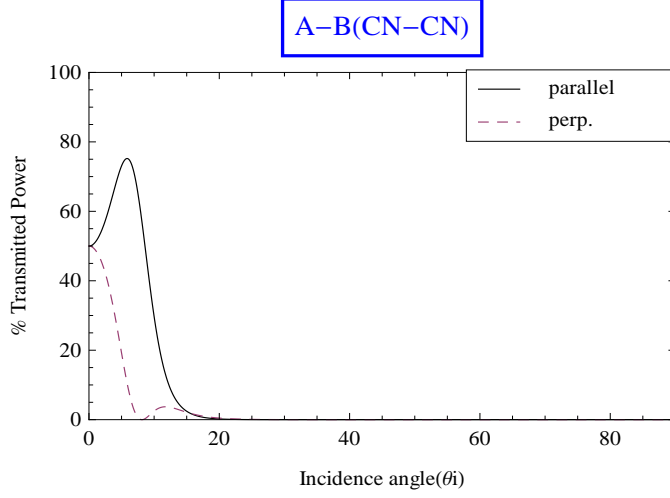


Figure 13:  $\epsilon_H = 1.6 \times 10^{-4}$ ,  $\epsilon_L = 2.5 \times 10^{-5}$ ,  $d_H = d_L = \lambda_0/4$ ,  $\mu_H = \mu_L = 10^{-5}$ ,  $\kappa_H = \kappa_L = 0.1$ ,  $f/f_0 = 1$

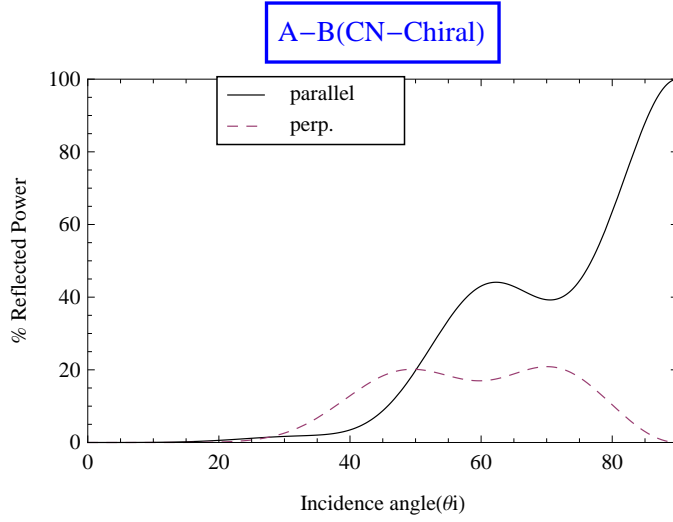


Figure 14:  $\epsilon_H = 1.6 \times 10^{-4}$ ,  $\epsilon_L = 2.5 \times 10^{-5}$ ,  $\mu_H = \mu_L = 10^{-5}$ ,  $d_H = d_L = \lambda_0/4$ ,  $\kappa_H = \kappa_L = 0.1$ ,  $f/f_0 = 1$

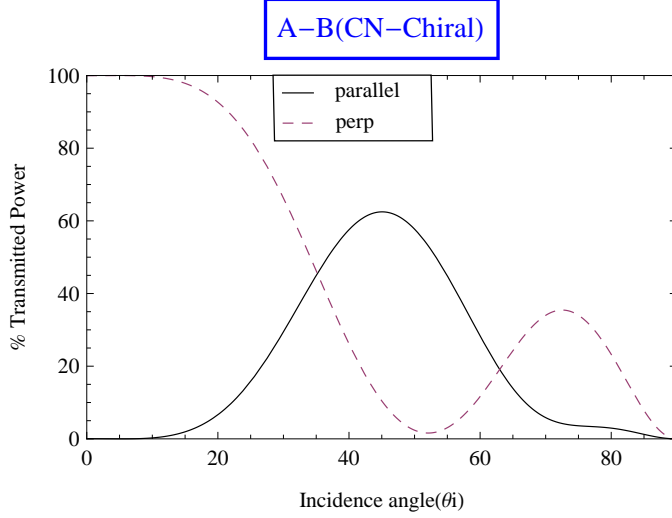


Figure 15:  $\epsilon_H = 1.6 \times 10^{-4}$ ,  $\epsilon_L = 2.5 \times 10^{-5}$ ,  $d_H = d_L = \lambda_0/4$ ,  $\mu_H = \mu_L = 10^{-5}$ ,  $\kappa_H = \kappa_L = 0.1$ ,  $f/f_0 = 1$

## 0.4 Conclusions

Behavior of planar multilayer periodic chiral nihility structures due to plane wave excitation has been studied using the transfer matrix method. Each multilayer structure is taken with periodicity two. First of all, behavior of CN-dielectric structure has been studied for the case of normal incidence. Total transmission as well as maximum rotation of power happens at 2THz. This stratified structure shows pronounced effects for oblique incidence. Total reflection of power for higher frequencies and small ripples, both in reflected and transmitted powers, for lower frequencies at oblique incidence are noted. Reflected power approaches to unity by increasing the value of angle of incidence and corresponding transmitted power has major part for small values of incidence angle.

Complete transparent behavior of CN-CN structure for all frequencies has been observed for normal incidence. Chirality introduces polarization rotation having maximum rotation at even harmonics. But for oblique incidence, total reflection from same structure has

been observed. At the end, behavior of CN-chiral structure has been studied and total rejection is observed for small incidence angles having major contribution of cross polarized components.



# Bibliography

- [1] N. Engheta and D. L. Jaggard, “Electromagnetic chirality and its applications”, IEEE Antennas and Propagation Social Newsletter, Vol. 30, 6-12, 1988.
- [2] D. L. Jaggard, A. R. Mickelson, and C. H. Papas, “On electromagnetic waves in chiral media”, Applied Physics, Vol. 18, 211-216, 1979.
- [3] S. Ougier, I. Chenerie, A. H Sihvola and A. Priou, “Propagation in bi-isotropic media: Effects of Different formalisms on the propagation analysis”, Progress In Electromagnetics Research, Vol. 9, 19-30, 1994
- [4] A. Lakhtakia, “On perfect lenses and nihility”, International Journal Infrared Millimeter Waves, Vol. 23, 339-343, 2002.
- [5] A. Lakhtakia and J. B. Goddes, “Scattering by nihility cylinder”, International Journal Electronics Communication, Vol. 61, 62-65, 2007.
- [6] S. Tretyakov, I. Nefedov, A. H. Sihvola, S. Maslovski, and C. Simovski, “Waves and energy in chiral nihility”, Journal of Electromagnetic Waves and Applications, Vol. 17, No. 5, 695-706, 2003.
- [7] A. H. Sihvola, “Advances in electromagnetics of complex media and metamaterials”, NATO Science Series, Vol. 89, 3-17, 2002
- [8] A. H. Sihvola, “Metamaterials in electromagnetics”, Metamaterials, Vol. 1, 211, 2007

- [9] A. N. Lagarkov, V. N. Kisel, V. N. Semenenko, “Wide-Angle Absorption by the Use of a Metamaterial Plate”, Progress In Electromagnetics Research Letters, Vol. 1, 35-44, 2008.
- [10] J. B. Pendry and R. David, “Reversing Light with Negative Refraction”, Physics Today, Vol. 57, No. 6, 37-44, 2004.
- [11] M. Shalaev, “Optical negative-index metamaterials”, Nature Photonics, Vol. 1, No. 1, 41-48, 2007.
- [12] S. Bassiri, C. H. Papas and N. Engheta, “Electromagnetic wave propagation through a dielectric-chiral interface and through a chiral slab”, Journal of the Optical Society of America A 5, 1450, 1988.
- [13] M. Tanaka and A. Kusunoki, “Scattering characteristics of stratified chiral slab”, IE-ICE Transactions on Electronics, Vol. E76-C 10, 1443 1993.
- [14] D. K. Kalluri and T. C. K. Rao, “Filter characteristics of periodic chiral layers”, Pure and Applied Optics 3, 231, 1994.
- [15] F. Ahmad, S. N. Ali, A. A. Syed, and Q. A. Naqvi, “Chiral and/or chiral nihility interfaces: parametric dependence, power tunneling and rejection”, Progress In Electromagnetics Research M, Vol. 23, 167-180, 2012.
- [16] J. F. Dong and C. Xu, “Surface polaritons in planar chiral nihility metamaterial waveguides”, Optics Communication, Vol. 282, 3899, 2009.
- [17] Q. A. Naqvi, “Planar slab of chiral nihility metamaterial backed by fractional dual/pemc interface”, Progress In Electromagnetics Research, Vol. 85, 381391, 2008.
- [18] A. Naqvi, F. Majeed, and Q. A. Naqvi, “Planar db boundary placed in a chiral and chiral nihility metamaterial”, Progress In Electromagnetics Research Letters, Vol. 21, 41-48, 2011
- [19] M. Khalid, S. Ahmed, A. A. Syed, and Q. A. Naqvi, “Electromagnetic response of a circular DB cylinder in the presence of chiral and chiral nihility metamaterials”, Progress In Electromagnetics Research M, Vol. 21, 253266, 2011.

- [20] M. Taj, A. Naqvi, A. A. Syed, and Q. A. Naqvi, “Study of focusing of a cylindrical interface of chiral nihility-chiral nihility media using Maslov’s method”, Progress In Electromagnetics Research Letters, Vol. 22, 181190, 2011.
- [21] C. Sabah, “Mirrors with chiral slabs”, Journal OF Optoelectronics and Advanced Materials Vol. 8, No. 5, 1918-1924, 2006.
- [22] C. Sabah, “Design of a terahertz polarization rotator based on a periodic sequence of chiral-metamaterial and dielectric slabs”, Progress In Electromagnetics Research, Vol. 124, 301-314, 2012
- [23] H. Cory and I. Rosenhouse, “Multilayered chiral filter response at oblique incidence”, Microwave and Optical Technology Letters 29, 192 ,2001.
- [24] C. Sabah and U. Savas, “Reflection and transmission coefficients of multiple chiral layers”, Science in China Series E: Technological Sciences Vol. 49, No. 4, 457467, 2006.
- [25] S. J. Orfanidis, “Electromagnetic Waves and Antennas”, ECE. Rutgers University, 2004.